Desalination and Water Treatment
www.deswater.com
5 (2009) 34–41
1944-3994/1944-3986 © 2009 Desalination Publications. All rights reserved

Performance evaluation and fouling characterisation of two commercial SWRO membranes

Ibrahim M. El-Azizi*, Robert G.J. Edyvean

Department of Chemical Process Engineering, The University of Sheffield, Mappin Street, Sheffield, S1 3JD, UK
Tel: +44 114 222 5776, +44 114 222 7506; Fax: +44 114 2225701; email: I.El-Azizi@sheffield.ac.uk; R.Edyvean@sheffield.ac.uk

Received 29 August 2008; Accepted 29 January 2009

ABSTRACT

The objectives of this study are to evaluate the performance of two different commercial seawater reverse osmosis (SWRO) membranes and to identify the causes of membrane failures. Membrane performances were evaluated by analysing the actual operating data and normalisation of permeate flow and salt passage. American Standards for Testing Materials (ASTM) and Homogenous solution diffusion (HSDM) standardisation methods were used. Comprehensive operating data for a period of 360 days were used to compare the accuracy of both methods. It was observed that the normalised permeate flow slightly decreased while normalised salt passage significantly increased during the operation period. The values of normalised permeate flows were identical by both standardisation methods, while the values of normalised salt passage were different. The standardisation methods showed that the performance deterioration of both RO membrane units is due to fouling. In order to determine the true identity of fouling two SWRO membrane elements were collected from the plant and subjected to membrane autopsies. The visual observation of unrolled membranes showed that the membrane surfaces and feed spacers were covered by loosely attached amorphous fouling material. Investigation by AFM found different types of fouling including inorganic, colloidal, and biofouling. The top surfaces of clean and fouled membranes were investigated by FTIR and XRD. FTIR results indicate that the major components of fouling materials are polysaccharides, silicate and hematite. XRD results indicate that the crystalline phase on the surfaces of both membranes was $CaCO_3$ scale as a mixture of calcite and aragonite.

Keywords: Desalination; Reverse osmosis; Membranes; Fouling; Autopsy

1. Introduction

Reverse osmosis (RO) membranes have been used in desalination of brackish and sea waters over the last three decades. The advantages of RO membrane technology are its ability to produce high quality water for drinking and industrial purposes, to reduce the size of treatment plant and to simplify water treatment processes. The most commercially available RO membranes are composed of a polyamide layer on top of a microporous polysulfone (PS) supported by a polyester non-woven backing layer. Fouling and degradation are the most serious problems that affect their performance. Fouling is a problem that requires expensive pretreatment and frequent chemical cleaning especially in the RO plants that use an open intake system. Fouling includes inorganic, organic, col-

*Corresponding author.

Presented at EuroMed 2008, Desalination for Clean Water and Energy Cooperation among Mediterranean Countries of Europe and the MENA Region, 9–13 November 2008, King Hussein Bin Talal Convention Center, Dead Sea, Jordan.

loidal and biological fouling which causes deterioration of product quality and quantity and an increase in energy consumption [1,2]. The early stages of fouling can be predicted using indirect methods such as measuring of silt density index (SDI), biological activity in raw and treated RO feed water, calculation of scaling potential and measuring of actual permeate flow, salt passage and differential pressure [3]. However, feed water quality, temperature and pressure can vary resulting in variation of product quality and quantity. As the temperature of RO feed water increases, osmotic pressure increases and the net driving pressure decrease. Moreover, increasing feed water temperature increases the pore size of the membrane causing an increase in salt and water permeability which deteriorates the quality of the product water [4]. Therefore, it is very important to normalize the operating data to determine the actual performance of RO membranes [5]. However, such indirect fouling observation methods have limitations in identifying the type and cause of fouling. The only reliable method of determining the true identity of membrane fouling is by membrane autopsy [6–9]. The term "autopsy" is used to describe a series of scientific tests and analysis on a used RO membrane element to reveal information about the causes and types of fouling that affect membrane performance [10,11]. Beside visual inspection the composition of fouling material can be determined using a variety of analytical techniques including x-ray photoelectron spectroscopy (XPS), X-Ray diffraction (XRD) and Fourier transform infrared spectroscopy (FITR) [12]. The ATR-FTIR spectra provide a way to determine the chemical composition of the membrane and fouling materials [13]. The composition and morphology of the fouling layer can be determined using scanning electron microscopy (SEM) and atomic force microscopy (AFM). AFM images provide a quantitative measurement of membrane surface roughness and the attachment of fouling material onto the membrane surface, while FTIR and XRD provide information on the components in the RO membranes and fouling materials [14–16]. Therefore, AFM, FTIR and XRD data offer direct information on the types and causes of the fouling. A fundamental understanding of the cause of membrane fouling and its prevention in full-scale SWRO desalination plants is very important for more effective and economical operation. The objectives of this study are to predict and identify fouling that cause membrane failure in a full scale SWRO desalination plant using the normalisation and membrane autopsy techniques.

2. Description of the RO plant

The Tajoura SWRO desalination plant is the largest RO plant in Libya and was designed to produce drinking and industrial waters. The total production capacity of the plant is 10,000 m^3/d [17,18]. The raw seawater is pre-treated using copper sulfate for disinfection, sulfuric acid for pH adjustment, ferric chloride for coagulation, dual-media filters, addition of anti-scalant and 5-micron cartridge filters prior to the RO membrane units. The plant consists of a seawater open intake, pre-treatment, two passes of RO membranes in two lines, post-treatment and product water storage. The first pass consists of four similar trains equipped with spiral wound SWRO membranes, a high pressure pump and recovery turbine. The permeate from the four trains flows to buffer tanks and is then pumped to the second pass. The second pass consists of two similar trains and each train consists of three stages equipped with BWRO membranes and a high pressure pump. A schematic diagram of the plant is shown in Fig. 1.

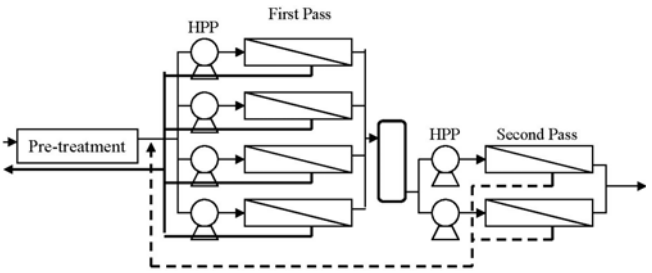

Fig. 1. Schematic flow diagram of a two-pass SWRO desalination plant.

3. Theory

Normalisation methods — The actual operating data such as feed pressure, water temperature and feed water conductivity can change with time causing changing in permeate quality and quantity. Therefore, it is necessary to normalise the actual operating data and compare the actual performance to the standard performance. Changes in the normalised parameters (permeate flow, salt passage and differential pressure) indicate the deterioration of the membrane performance. The ASTM mathematical model consists of two main parameters: normalised permeate flow and normalised salt as shown in Eqs. (1) and (2).

$$NPF = \frac{NDP_s TCF_s}{NDP_a TCF_a} Q_{pa} \quad (1)$$

$$NSP = \frac{NDP_a C_{fcs} C_{fa}}{NDP_s C_{fca} C_{fs}} S_{pa} \quad (2)$$

The HSDM method, which is derived from fundamental diffusion theory, can also be used to normalize the

actual operating data of NF and RO membranes [19]. The normalisation of permeate flow using the HSDM is identical to the ASTM method [Eq. (1)]. However, by the HSDM the normalised salt passage, which is a ratio of diffusion of salt flux divided by water flux, is calculated using Eq. (3).

$$SP = \frac{K_s C_{fca}}{K_w(\Delta P - \Delta\Pi)C_{fa}} \quad (3)$$

The water and salt permeability coefficients can be calculated using Eqs. (4) and (5).

$$K_w = \frac{J_w}{(\Delta P - \Delta\Pi)} \quad (4)$$

$$K_s = \frac{J_s}{(\Delta C)} \quad (5)$$

4. Materials and methods

4.1. Membrane autopsy

To investigate the causes of deterioration of plant performance and to determine the true identity of fouling, two SWRO membrane elements were removed from the installation and subjected to autopsy. The elements were covered by sterilised plastic bags and stored at 4°C until analysis to preserve the original biomass composition as present under the operation conditions. In the laboratory the end caps and outer casing of the membrane elements were inspected and removed. The membrane elements were unrolled for visual inspection and testing following the autopsy standard procedures [5–9].

4.2. Microbiological investigation

The microbiological analysis of fouling material was carried out according to the method used by Schneider et al. [20]. Fouled membrane samples of a known area (5×5 cm) were cut off from membrane sheets and transferred into test tubes containing 10 ml of sterile seawater and vortexed. Serial dilutions were carried out to determine the number of bacteria (expressed in colony forming units per area (cfu/cm^2) on R_2A agar. A 0.1 ml sample was spread on R_2A medium Petri dishes. The plates were incubated at 32ºC and counted periodically until the number of colonies stabilised. R_2A medium was selected for its low nutrient content, moderate incubation temperature, long incubation time and suitability for recovery of stressed and chlorine-tolerant bacteria [21].

4.3. Atomic force microscopy (AFM)

A nanoscope III atomic force microscope (Digital Instruments, USA) was used to investigate the surface morphology of clean and fouled RO membrane samples. Clean membrane samples were rinsed and soaked in distilled water for 24 h. Both clean and fouled membrane samples were transferred into clean Petri dishes and dried in a laminar flow cabinet prior to AFM investigation. Standard nanoprobe silicon (Si) cantilevers (model OMCL-AC160TS-E) were used. A tapping mode in the dry state was used. Small pieces of membrane were cut off from the dried membrane samples and placed on a stainless steel disc and investigated by AFM.

4.4. ATR–FTIR

Attenuated total reflection–Fourier transform infrared spectroscopy (ATR–FTIR) was used to investigate the functional groups of clean and fouled thin film composite SWRO membranes. FTIR analysis was conducted using a Perkin Elmer FTIR spectroscope. Clean and fouled membrane samples were prepared by the same procedure mentioned in Section 4.3. Previously dried membrane samples (3×3 cm) were pressed against each side of a germanium (GE) reflection element (6 mm, 45º). All spectra (100 scan at 4 cm^{-1} resolution) were recorded at 25ºC.

4.5. XRD of membrane samples

The crystalline phases of fouling material deposited on the surface of both SWRO membranes were analysed by XRD. The XRD was carried out to determine the chemical nature of the scales deposited on the surface of RO membranes and to determine if the $CaCO_3$ scale is present as calcite, aragonite or a mixture of both. Clean and fouled membrane samples were prepared by the same procedure mentioned in Section 4.3. A Philips X-Ray diffract meter was used to scan clean and fouled RO membrane samples over the range of 5–80° at scan speed of 1°/min and a step size of 0.02°.

5. Results and discussion

5.1. Performance evaluation of fluid systems and Toray RO membrane units

Performances of Fluid Systems and Toray membrane units were evaluated by analysing the actual operating data for a period of 360 days. The parameters used were permeate flow, permeate concentration and differential pressure. It was noticed that the operating pressure was increased gradually to avoid the decline in production

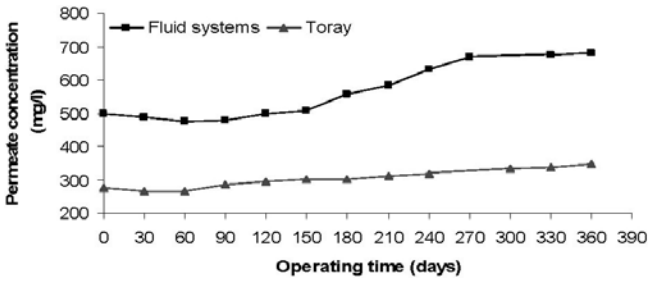

Fig. 2. Actual permeate concentration vs. operating time for the Fluid Systems and Toray membrane units.

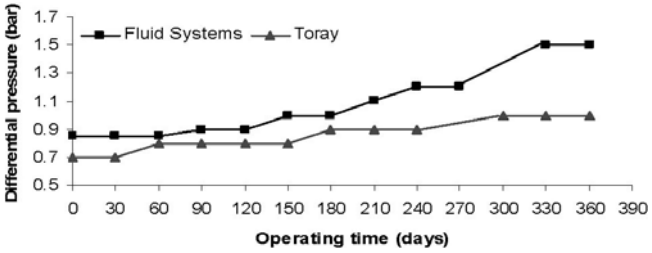

Fig. 3. Actual differential pressure vs. operating time for the Fluid Systems and Toray membrane units.

rate. After 1 year of operation both membrane systems had stable permeate flow within the design values. The permeate concentration of both membrane units increased steadily with operating time by about 27% and 21% respectively (Fig. 2) , while the differential pressure increased by about 43% and 30 % respectively (Fig. 3).

From Figs. 2 and 3 it can be seen that the permeate concentration and differential pressure values of the Fluid Systems membrane unit are higher than the Toray membrane unit due to differences in membrane specifications. Actual performances of RO membrane systems are not steady and operating data fluctuated with time; therefore, permeate flow and salt passage have to be normalised. The normalised permeate flow and salt passage calculated using Eqs. (1)–(4) of the ASTM and HSDM are shown in Figs. 4 and 5 respectively.

It can be seen from Fig. 4 that normalised permeate flows for both RO membrane units follow similar patterns. The methods are identical in normalisation of permeate flow and difference in normalisation of salt passage (Fig. 5). Normalised permeate flow of the both membrane units were initially higher than the actual permeate flow and decreased gradually during the first 6 months of operation. This can be attributed to the effect of the pressure correction factor [22]. After 270 days of operation normalised permeate flow of both units decreased by about 13% and 7% respectively, while the normalised salt passage increased steadily with operating time by about 25% in both RO membrane units. According to these results it can be concluded that the fouling is the main reason for performance deterioration of the RO membrane

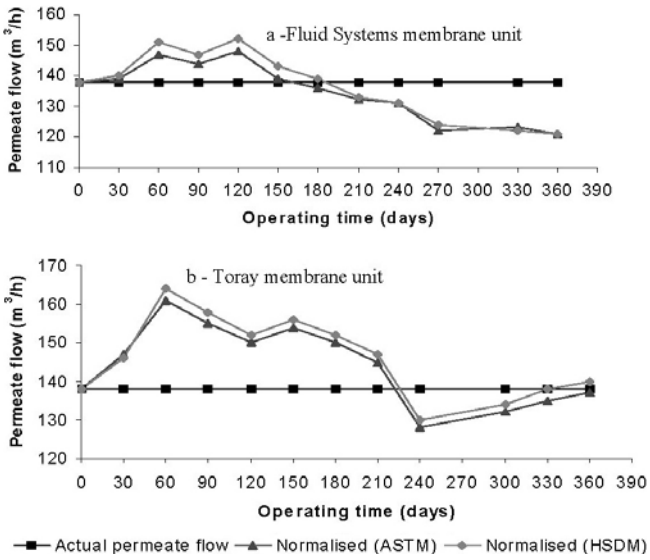

Fig. 4. Actual and normalised permeate flow vs. operating time for (a) Fluid Systems and (b) Toray SWRO membrane units.

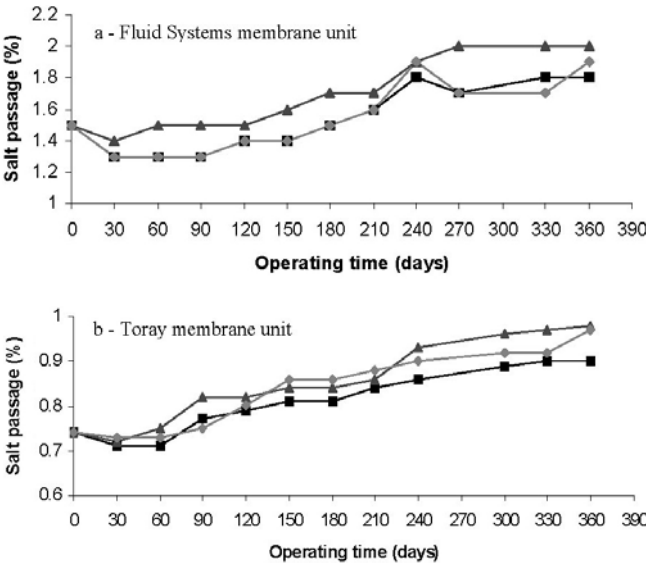

Fig. 5. Actual and normalised salt passage vs. operating time for Fluid Systems and Toray SWRO membrane units.

units in the plant. However, performance normalisation methods can not determine the true identity and causes of fouling and are used to determine when chemical cleaning should be implemented to prevent irreversible fouling. It is difficult to detect the early development of membrane fouling in the RO membrane systems by monitoring long-term performance because fouling is cumulative in nature and builds up with operating time [23]. Therefore, membrane autopsy is the only reliable method for determining the true identity of membrane fouling.

5.2. Membrane autopsy

Membrane autopsies were carried out on two 8" SWRO membranes from Fluid Systems and Toray. Both RO membranes were visually inspected for evidence of damage. No evidence of telescoping or damaging of outer casing was seen. The membrane elements were unrolled and the membrane surfaces, feed and permeate spacers were visually inspected. Creep near the glue lines was observed in Fluid Systems membranes but not in Toray membranes. The surfaces of both membranes were covered by reddish brown fouling deposits. The presence of creep near glue lines is due to high differential pressure, water hammering and/or a manufacturing problem. The deposits on the membrane surfaces of both membranes were highly amorphous and can be easily removed by swabbing and water flushing.

5.3. Microbiological enumeration

Microbiological analyses were carried out on known areas (5×5 cm) of membrane surface using the plate count method in R_2A agar. The number of microorganisms that are present are expressed as colony forming units per area (cfu/cm^2) (Table 1).

From Table 1 it can be seen that the bacterial counts on the Fluid Systems membranes is slightly higher. Darton [8] reported that the performance of RO membrane systems would not be affected if the bacterial count remains below 10^4cfu/cm^2 because the biofilm is stable in this condition and many plants work satisfactorily with such a biofilm. Where the bacterial count exceeds 10^5 cfu/cm^2, the biofilm is considered to be producing sufficient polysaccharides to become problematic in RO membrane systems. The polysaccharide material can act as a trap for other fouling materials and increase the potential of composite fouling. The bacterial count in the fouling material was found to be 10^5 cfu/cm^2, and biofilm is therefore one of the operational problems in both RO membrane units.

5.4. Atomic force microscope results

The surface morphologies and membrane roughness of clean and fouled membranes were investigated using AFM. Both clean RO membranes have rough surfaces with peak-and-valley structures (Fig. 6). These could trap

Table 1
Bacterial count (cfu/cm^2) of membrane samples

Membrane samples	Fouling material (cfu/cm^2)
Fluid Systems	1.1×10^5
Toray	6.2×10^4

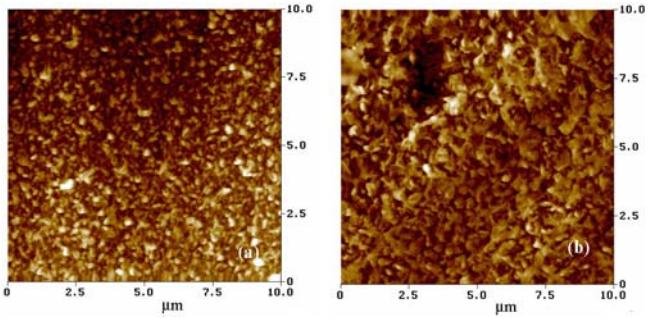

Fig. 6. AFM images of clean Fluid Systems (a) and Toray (b) SWRO membranes.

fouling materials which may cause a severe fouling. The AFM images of the fouled membranes were markedly different from those of clean membranes (Fig. 7). Similar fouling materials, amorphous in nature, were detected on both membranes.

From Fig. 7 (images a and c) it can be seen that both membrane surfaces are completely covered by fouling material. Long needles of crystals were observed on the surface of the fouled Toray membrane (see Fig. 7c), indicating precipitation of $CaSO_4$. The calcite form of $CaCO_3$ with rhombohedral morphology and sharp straight edges is observed on the surface of both membranes (Fig. 7b and d) while, rod-shaped microbes were detected on the surface of Toray membranes (see Fig. 8b). It seems that when the fouling layer reaches a certain thickness, further materials such as crystals and extracellular polymeric substances, are deposited on the surface of fouling layer.

The presence of $CaCO_3$ scaling on the surfaces of both RO membranes is attributed to the high pH of RO feed water and/or the high salt concentration on the membrane surface due to fouling. Fouling limits back diffusion of solute from the membrane surface to the bulk solution and increases the salt concentration at the membrane surface [24,25]. Tzotzi [26], in his study of $CaCO_3$ scale formation in RO and NF membranes, attributed the domination of calcite crystals to solution pH and/or higher supersaturation level of $CaCO_3$. From Fig. 8 one can see that the structure of calcite crystals increases in size with regular and deformed shapes in which they agglomerate, forming a layer of blocks and/or plates blocking the membrane surface.

Chen [27] investigated the effect of Mg^{2+} on $CaCO_3$ formation found that with increasing Mg^{2+} concentration in solution the formation of calcite crystals with distorted edges is increased and the cubical and/or rhombohedral structure of crystals is changed. He observed that at 0% concentration of Mg^{2+} in solution all calcite crystals are perfect in structure; however, with increasing Mg^{2+} the structure of $CaCO_3$ crystals is distorted. The Mg^{2+} ions are possibly adsorbed on the surface of calcite crystal and cause the distortion of the edge of calcite crystal and

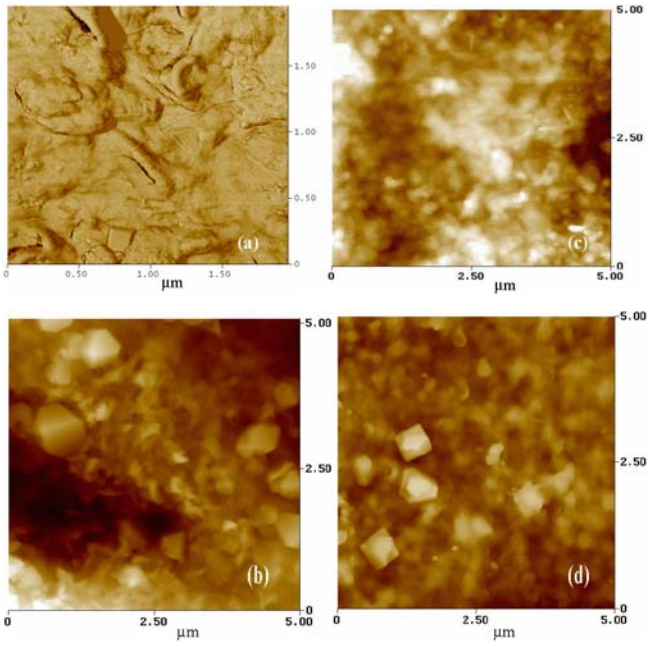

Fig. 7. AFM images of fouled Fluid Systems (a and b) and Toray (c and d) SWRO membranes by calcium carbonate in the calcite form.

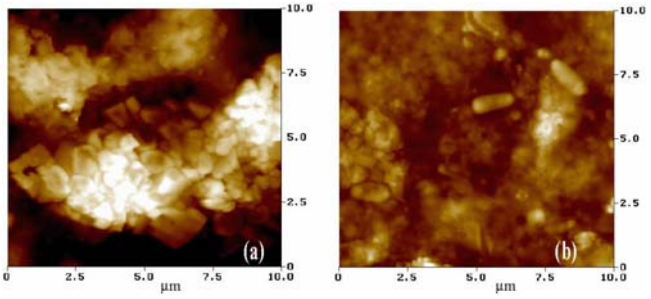

Fig. 8. AFM images of blocking layer of calcite crystals on the surface of Fluid Systems (a) and Toray (b) SWRO membranes.

Table 2
Surface roughness of clean and fouled Fluid Systems and Toray SWRO membranes

Membrane type	*Ra* (nm)	*Rms* (nm)
Fluid Systems (new)	41.251	51.692
Fluid Systems (fouled)	98.466	143.29
Toray (new)	49.144	63.705
Toray (fouled)	87.748	104.55

formation of crystals with rough surfaces. The same results were observed on the surface of Fluid Systems and Toray SWRO membranes which can be attributed to the high concentration of Mg^{2+} in the RO feed water.

The AFM allows measurement of the arithmetic (*Ra*) and the geometric mean (*Rms*) of surface roughness. Table 2 presents the *Ra* and *Rms* values for clean and fouled membranes. The AFM images and surface roughness calculation showed that the clean Toray SWRO membrane has a rougher surface compared to the Fluid Systems membrane. However, the surface roughness of the fouled Fluid Systems membrane is higher than the Toray membrane. A possible reason is that the Toray membranes were placed after refurbishment of pretreatment systems in the plant; however, AFM images and surface roughness calculation indicate that the fouling potential in the plant is still high even after the refurbishment process.

5.5. ATR–FTIR spectroscopy results

ATR–FTIR spectroscopy is a very useful tool for determining the chemical composition of the RO membrane and fouling material. Attenuated total reflection (ATR) offers the possibility of investigating the chemical composition of smooth surfaces such as RO membranes without any sample preparation and thus in the undisturbed state. The IR beam can penetrate through the membrane or fouling layer and gives a spectrum of the average composition of this layer. Therefore, the FTIR spectra of clean and fouled Fluid Systems and Toray SWRO membranes were investigated to identify the chemical groups of RO membrane and fouling materials (Fig. 9).

The spectra of clean and fouled RO membranes were compared. It was observed that both clean SWRO membranes have similar spectra where the majority of strong peaks are located in the amide and carbohydrates regions (1750 and 700 cm^{-1}). These peaks are not present in the spectrum of the fouled RO membranes and can not be detected by FTIR because the fouled layer appears to be more than 1 µm thick which is the maximum the infrared light wave can penetrate. An expanded region of FTIR spectra between 1700 and 700 cm^{-1} for clean and fouled RO membranes is shown in Fig. 10.

The strong peaks in the spectra of fouled membranes indicate that the fouling materials are polysaccharides, hematite and/or silicate (1038 and 930 cm^{-1}) and proteins (1570–1640 m^{-1}) [28,29]. Cho et al. [30] attribute FTIR absorption in this region to polysaccharides, while Howe et al. [11], attribute this absorption to silicate impurities. Pei Xu et al. [31] attributes this absorption in the carbohydrate region to polysaccharides, silicate and colloids. The FTIR results suggest that the deposits on the surfaces of both RO membranes contain, polysaccharides, silicate clay minerals and iron compounds which pass through the pretreatment systems and accumulate on the membrane surfaces.

5.6. XRD results

The spectra of clean and fouled membrane samples

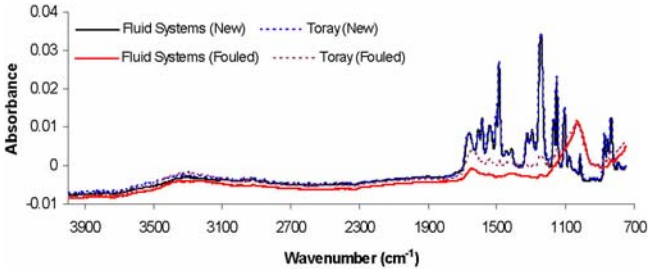

Fig. 9. FTIR spectrum of clean and fouled Fluid Systems and Toray SWRO membranes.

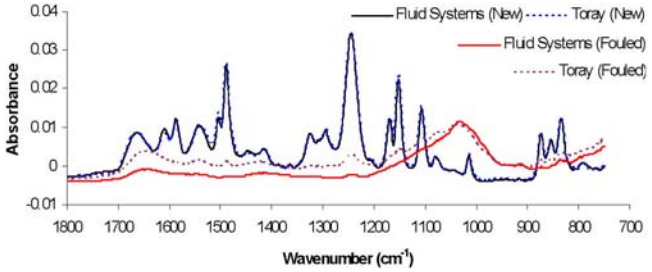

Fig. 10. Expanded FTIR spectrum of clean and fouled Fluid Systems and Toray SWRO membranes.

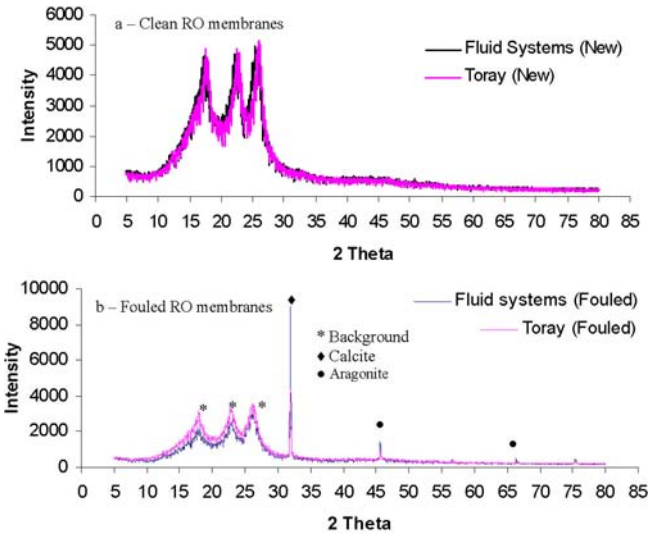

Fig. 11. XRD spectra of clean (a) and fouled (b) Fluid Systems and Toray SWRO membranes.

show similar peak patterns (Figs. 11a and b). However, differences in the peak heights indicated that the concentration of $CaCO_3$ scale is higher in the Fluid Systems membrane compared to the Toray membrane.

Calcium carbonate scale can form on the membrane surface as calcite and aragonite where aragonite tends to form in solutions containing magnesium [32]. The X-ray patterns of fouled membranes were found to contain several crystalline peaks at 2θ values of approximately 33.3°, 46.3° and 66.5°, representing the presence of the $CaCO_3$ scale as both calcite and aragonite. The calcite peak at 2θ values of approximately 33.3° was found to be higher on the Fluid Systems membranes than that on the Toray membrane. The XRD results were confirmed by AFM observations in which $CaCO_3$ scaling was found to be hard and tenacious. Both fouled membranes were chemically cleaned by hydrochloric acid (HCl) after which the $CaCO_3$ peaks disappear from the spectra, indicating that HCl has excellent removal ability for $CaCO_3$ scale.

6. Conclusions

ASTM and HSDM are useful methods for evaluation of RO membrane performance. The two RO membrane units show permeate flow higher than the design in the first 6 months; then it decreases, while the normalised salt passage and differential pressure increased significantly with operational time due to fouling. The identity of fouling was determined using membrane autopsy techniques. The visual inspection of the unrolled SWRO membranes revealed a heavy brownish-reddish foulant layer on the surfaces and feed spacers of both membranes. Presence of creep near the glue lines of Fluid Systems membrane may be attributed to high deferential pressure or water hammering and/or possibly due to a manufacturing problem.

The deposits on both membranes are predominantly amorphous in nature and can be easily removed by swabbing and water flushing. The biological growth on the membrane surfaces with bacterial count 10^5 is a problem for the operation of the RO membrane units. Membrane surface examination by AFM shows that the membrane surfaces are covered by a thick fouling layer which contains different foulants. ATR–FTIR investigation of clean and fouled SWRO membrane samples shows new peaks at 1038 and 930 cm^{-1} in the fouled RO membrane corresponding to polysaccharides, hematite and silicate. XRD results suggest the formation of $CaCO_3$ crystals on the surfaces of both membranes as a calcite and aragonite. AFM, ATR–FTIR and XRD provide valuable information about about types and cause of fouling that can lead to membrane failure.

From the results, the following recommendations can be made:

- Regular monitoring of pretreatment and RO membrane systems in real time operation to predicate fouling in early stages is required.
- Regular normalisation of permeate flow and salt passage data to determine when chemical cleaning of the RO membranes should be implemented.
- Adjustment of seawater pH and the use of an effective antiscalant is necessary.
- Regular flushing of RO membranes during plant shutdown is required.

7. Symbols

C — Concentration gradient = $(C_{fc} - C_p)$, mg/l
C_p — Permeate concentration, mg/l
C_{fa} — Feed concentration, mg/l
C_{fca} — Actual log mean of feed–concentrate concentration, mg/l
C_{fcs} — Standard log mean of feed–concentrate concentration, mg/l
J_s — Solute flux, m/h
J_w — Water flux, $m^3/m^2.h$
K_s — Salt permeability coefficient, m/h
K_w — Water permeability coefficient, $m^3/m^2.hr.bar$
NPF — Normalised permeate flow, m^3/h
NDP_a — Actual net driven pressure, bar
NDP_s — Standard net driven pressure, bar
NSP — Percent normalised salt passage, %
P — Pressure gradient = $(P_f + P_c/2)$, bar
Q_{pa} — Actual permeate flow rate, m^3/h
SP_a — Actual percent salt passage, %
TCF_a — Actual temperature correction factor
TCF_s — Standard temperature correction factor
Π — Osmotic pressure gradient = $\Pi_{fc} - \Pi_p$, bar

Acknowledgements

Thanks to the Renewable Energy and Water Desalination Research Centre and the Tajoura Seawater Desalination Plant, Libya, for the support of this project. Thanks to Dawn Bussey, Robert Bachmann and Jesus Ojeda for their assistance in AFM and FTIR.

References

[1] M.F.A. Goosen, S.S. Sablani, H. Al-Hinai, S. Al-Obeidani, R. Al-Belushi and D. Jackson, Fouling of reverse osmosis and ultrafiltration membrane: a critical review, Sep. Sci. Technol., 29 (2004) 2262–2298.
[2] Q. Li and M. Elimelech, Synergistic effect in combined fouling of a losse nanofiltration membrane by colloidal materials and natural organic matter, J. Membr. Sci., 278 (2006) 72–82.
[3] L.Y. Dudely and E.G. Darton, Pretreatment procedures to control boigrowth and scale formation in membrane systems, Desalination, 118 (1997) 11–20.
[4] N.M. Al-Bastaki and H.L. Al-Qahtani, Assessment of thermal effects on the reverse osmosis of salt/water solution by using a spiral woumd polyamide membrane, Desalination, 99 (1994) 159–168.
[5] H. Huiting, J.W.N.M. Kappelhof and T.G.J. Bosklopper, Operation of NF/RO plants: from reactive to proactive, Desalination, 139 (2001) 183–189.
[6] F.H. Butt, F. Rahman and U. Baduruthamal, Characterization of foulants by autopsy of RO desalination membranes, Desalination, 114 (1997) 51–64.
[7] F.H. Butt, F. Rahman and U. Baduruthamal, Identification of scale deposits through membrane autopsy, Desalination, 101 (1995) 219–230.
[8] T. Darton, U. Annunziata and F. del Vigo Pisano, Membrane autopsy helps to provide solution to operational problems, Desalination, 167 (2004) 239–245.
[9] L.Y. Dudely and E.G. Darton, Membrane autopsy — a case study, Desalination, 105 (1996) 135–141.
[10] S. Gallego Lopez, F. del Vigo Piasno and J. Shango Munoz, Membrane autopsies: helps to provide solutions to operational problems in reverse osmosis plants, Water Sci. Technol., 5 (2005) 129–135.
[11] A. Mohamed, F. Mohamed, A. Al-Amoudi, A.T.M. Jamaluddin and A.M. Hassan, Performance restoration, autopsy and analysis of five different commercial SWRO membranes, IDA World Congress on Desalination and Water Reuse, Spain, 1997.
[12] K.J. Howe, K.P. Ishida and M.M. Clark, Use of ATR/FTIR spectrometry to study fouling of microfiltration membranes by natural waters, Desalination, 147 (2002) 251–255.
[13] C.Y. Tang, Y.N. Kown and J.O. Leckie, Probing the nano-scales of reverse osmosis membranes—A comprehensive characterization of physicochemical properties of uncoated and coated membranes by XPS, TEM, ATR-FTIR, and streaming potential measurements, J. Membr. Sci., 287 (2007) 146–156.
[14] A.N. Hilal, W. Mohammad, B. Atkin and N.A. Darwish, Using atomic force microscopy towards improvement in nanfiltration membranes properties for desalination pre-treatment: a review, Desalination, 157 (2003) 137–144.
[15] V. Freger, H. Gilron and S. Blefer, TFC polyamide membranes modified by grafting of hydrophilic polymers: an FT-IR/AFM/TEM study, J. Membr. Sci., 209 (2002) 283–292.
[16] R.T. Bachmann and R.G.J. Edyvean, AFM study of the colonization of stainless steel by *Aquabacterium commune*, Inter. Biodeter. Biodegrad., 58 (2006) 112–118.
[17] A.A. Abufayed, Performance characteristics of cyclically operated seawater desalination plant in Tajoura, Libya, Desalination, 139 (2001) 131–132.
[18] I. El-Azizi and A. Omran, Design criteria of 10,000 m^3/d SWRO desalination plant of The Tajoura, Libya, Desalination, 153 (2003) 273–279.
[19] Z. Yu and J.S. Taylor, Assessment of ASTM D 4516 for evaluation of reverse osmosis membrane performance, Desalination, 180 (2005) 231–244.
[20] R.P. Schneider, L.M. Ferreira, P. Binder and J.R. Ramos, Analysis of foulant layer in all elements of an RO trains, J. Membr. Sci., 261 (2005) 152–162.
[21] E.M. Vrijenhoek, S. Hong and M. Elimelech, Influence of membrane surface properties of initial rate of colloidal fouling of reverse osmosis and nanofiltration membranes, J. Membr. Sci., 188 (2001) 115–128.
[22] M. Safar, M. Jafar, M. Abdel-Jawad and S. Bou-Hamad, Standardization of RO membrane performance, Desalination, 118 (1998) 13–21.
[23] M.A. Saad, Early discovery of RO membrane fouling and real-time monitoring of plant performance for optimizing cost of water, Desalination, 165 (2004) 183–191.
[24] M. Elimelech, X. Zhu, A.E. Childress and S. Hong, Role of membrane surface morphology in colloidal fouling of cellulose acetate and composite aromatic polyamide reverse osmosis membranes, J. Membr. Sci., 209 (2002) 283–292.
[25] E.M.V. Hoek and M. Elimelech, Cake-enhanced concentration polarization: A new fouling mechanism for salt-rejection membranes, Environ. Eng. Soc., 37 (2003) 5581–5588.
[26] Ch. Tzotzi, T. Pahiadaki, S.G. Yiantsios, A.J. Karabelas and N. Andritsos, A study of $CaCO_3$ scale formation and inhibition in RO and NF membrane processes, J. Membr. Sci., 296 (2007) 171–184.
[27] T. Chen, A. Neville and M. Yuan, Assessing the effect of Mg^{++} on $CaCO_3$ scale formation-bulk precipitation and surface deposition, J. Membr. Sci., 175 (2005) 1341–1347.
[28] H.L. Yang, C. Huang and J.R. Pan, Characteristic of RO foulants in a brackish water desalination plant, Desalination, 220 (2008) 353–358.
[29] J. Schmitt and H.-C. Flemming, FTIR-spectroscopy in microbial and material analysis, Intern. Biodeter. Biodegrad., 41 (1998) 1–11.
[30] J. Cho, G. Amy, J. Pellegrino and Y. Yoon, Characterization of clean and natural organic matter (NOM) fouled NF and UF membranes, and foulants characterization, Desalination, 118 (1998) 101–108.
[31] P. Xu, J.E. Drewes, T.-U. Kim, C. Bellona and G. Amy, Effect of membrane fouling on transport of organic contaminants in NF/RO membrane applications, J. Membr. Sci., 279 (2006) 165–175.
[32] G. Falini, M. Gazzano and A. Ripamonti, Crystallization of calcium carbonate in presence of magnesium and polyelectrolytes, J. Crystal Growth, 137 (1994) 577–584.